# Bulletin of the Mineral Research and Exploration

BULLETIN OF THE
MINERAL RESEARCH AND EXPLORATION

CONTENTS

# Rare earth elements and yttrium geochemistry of the geothermal fields in the Eastern Black Sea Region (Ordu, Rize, Artvin), NE Turkey

Esra HATİPOĞLU TEMİZEL[a*] , Fatma GÜLTEKİN[a] and Arzu FIRAT ERSOY[a]

[a]Karadeniz Techincal University, Department of the Geological Engineering, 61080 Trabzon, Turkey.

## ABSTRACT

In this study, behavior and migration processes of rare earth elements (REEs) were determined in the thermal and cold waters of the geothermal fields in the Eastern Black Sea Region. The temperatures of the geothermal waters are between the range of 38 and 60 °C. The water types are $Na\text{-}Ca\text{-}SO_4$ for Sarmaşık (Ordu) field, $Na\text{-}Ca\text{-}HCO_3$ for Ikizdere (Rize) field, $Na\text{-}Ca\text{-}CO_3\text{-}SO_4$, for Ayder (Rize) field and $Na\text{-}HCO_3\text{-}Cl$ for Savsat (Artvin) field. All geothermal fields are in alkaline geothermal character (pH: 7-9.3) and have very low REE + Y concentrations, slightly significant Ce contens and significantly positive Eu anomalies (except for Ayder geothermal field). REE+Y content, fractionation and positive Eu anomalies of the investigated water are controlled by water/rock ratio, pH and minerals in the host rocks. According to the thermodynamic calculations, it was determined that the mobility of the REEs in geothermal fields were mainly controlled by $Ln^{3+}$, $LnOH^{2+}$, $LnCl^{2+}$, $Ln(SO_4)_2^-$, $LnSO_4^+$, $LnHCO_3^{2+}$, $Ln(CO_3)_2^-$ and $LnCO_3^+$ complexes.

## 1. Introduction

Rare earth elements (REE) are compatible group elements that have similar physicochemical properties with atomic numbers ranging from 57 to 71 (La-Lu). Yttrium exhibits chemical behaviors similar to REE and is used in geochemical studies. In recent studies related to the hydrothermal systems conducted by many researchers, significant information about the geochemical behaviors of waters were determined like the change in chemical composition of geothermal waters during underground circulation by examining the behavior of REE and Y (REE+Y), the sources of this composition, alteration, secondary mineral deposition conditions, condition and motion of particulate materials (Hass et al., 1995; Bau and Dulski, 1999; Embley et al., 2007; Craddock and Batch, 2010; Göb et al., 2013, Shakari, 2015; Bragin et al., 2018).

The events such as the rate of interaction between the water and host rock, the absorption processes and chemical complexation reactions in hydrothermal systems affect the distribution models of REE. As known, the equilibrium and decomposition conditions of REE bearing minerals cause the mobility and release of REE during the alteration of host rock. The solubility of REE depends on the presence of anionic ligands, which complicates and stabilizes these elements in the groundwater. Therefore, the chemical speciation calculations based on the thermodynamic principles can reveal more information about the chemical processes of REE+Y in the geothermal waters (Wood, 1990). REE+Y are used to understand the processes such as the water-rock-magmatic gas interaction, primary mineral dissolution, secondary mineral deposition (Bragin et al., 2018).

In the Eastern Black Sea Region, there are many studies on the mineralogy and petrography of the rocks in the areas where volcanic and magmatic rocks generally outcrop (Özbeşikçi et al., 1981; Gedik et al., 1992; Göksu, 1996; Temizel, 2002; Karslı et al., 2004; Arslan and Aslan, 2006; Temizel et al., 2012; Evcimen and Karslı, 2012). NE-SW trending strike-slip faults, which control the flow of hot water to the surface at the same time form the catchment routes. The General Directorate of Mineral Research and Exploration (MTA) and the other researchers have conducted many researches in their close vicinities to investigate and use these hot springs (Kartal, 1972; Büyük, 1978; Terlemez and Yılmaz, 1980; Erzenoğlu and Tangaç, 1986; Gürsel, 1991; Kara, 1997; Uzel et al., 1998; Gündüz, 1999; Fırat Ersoy, 2001; Akkuş et al., 2005). Unlike the studies carried out in the literature, the REE+Y contents and fractionation of the Sarmaşık geothermal field (SGF), Ayder geothermal field (AGF), İkizdere geothermal field (İGF) and Şavşat geothermal field (ŞGF) waters were detected in this study. In addition to these, the calculation of chemical speciation of the waters and the geochemical processes controlling the REE+Y contents in the water were also evaluated.

## 2. Material and Methods

The field studies were conducted between April 2016 and October 2017 as geological studies, in-situ measurement and sampling. The sampling was carried out in 20 locations as being 4 hot spring wells, 2 hot springs, 6 cold springs and 8 surface waters. During the in-situ measurements at the water sampling points, the measurements of T (temperature), EC (electrical conductivity), pH, TDS (Total Dissolved Solids) were made by YSI-556 model multi-parameter measuring instrument.

The probes used during measurements were kept by being washed with pure water before and after each measurements and were run with buffer solutions after daily calibrations before each field study. In order to determine the major anion-cation and trace element contents of the waters, the sampling was made with 500 mL polyethylene bottles.

The chemical and REE+Y analyzes of water samples were carried out in the Water Chemistry Laboratory of the Hydrogeology Engineering Department of Hacettepe University (Ankara, Turkey)

by the ion chromatography technique and Inductively Coupled Plasma – Mass Spectrometry (ICP-MS) methods, respectively. The major cations ($Ca^{2+}$, $Mg^{2+}$, $Na^+$ and $K^+$) were determined by the $Cl^-$ and sulfate ion chromatography system. The alkalinity was however determined by the standard titration method. $SiO_2$ was analyzed by the spectrophotometric method. The ion balance error of the analyzes is below 5%. The rock geochemical analyzes were performed using Inductively Coupled Plasma – Mass Spectrometry (ICP-MS) in the ACME Laboratory (Canada).

The selected complexes of REE ($Ln^{3+}$, $LnCO_3^+$, $Ln(CO_3)_2^-$, $LnCl^{2+}$, $LnSO_4^+$, $LnHCO_3^{2+}$, $LnOH^{2+}$, $LnO^+$, $LnO_2^-$ ve $LnO_2H^*$; Ln represents any of the Lantanides) were calculated by using the database of the thermodynamic parameters in the Visual MINTEQ software (Gustafsson, 2012) . It was calculated by using database. The modeling process was carried out for the actual groundwater composition by using the temperature and pH values measured in water in the atmospheric pressure. The major ions, Fe, Mn, Al and REE+Y were used in the calculations. Ce and Eu anomalies ($Ce/Ce^*= Ce_{CN}/(La_{CN}*Pr_{CN})^{0.5}$) were calculated using ($Eu/Eu^*=Eu_{CN}/(Sm_{CN}*Gd_{CN})^{0.5}$) equations (CN: Chondrite normalized value (Sun and McDonough, 1989)).

## 3. Geological and Hydrogeological Structures

The Eastern Black Sea Region located to the east of Turkey is geologically called as the eastern Pontide tectonic unit (Ketin, 1966). The Pontides are divided into two as the Western Pontides and Eastern Pontides in the west and east of Samsun (Özsayar et al., 1981). The tectonic unit of the Eastern Pontides is divided into two zones as; the "North" and "South" with the Ardanuç-İspir-Kemaliye-Reşadiye border by Özsayar et al. (1981). While the magmatic and volcano-sedimentary rocks are dominant in the Northern Zone of the Eastern Pontide, the sedimentary rocks are dominant in the Southern Zone. SGF, İGF, AGF and ŞGFs studied within the framework of this study are located in the Northern Zone of the Eastern Pontides. The units belonging to the Paleozoic, Mesozoic and Cenozoic periods outcrop in the northern zone (Figure 1). The Paleozoic granitoids form the oldest unit in the Eastern Pontides. These units are unconformably overlain by the Jurassic volcanics and volcaniclastics. The Late Cretaceous in the region is represented mainly by the volcanic (basalt, andesite and pyroclastics)

and clastic sedimentary rocks (sandstone, siltstone and mudstone). The Late Cretaceous granitoids were emplaced by cutting these units. The age of the clastic sedimentary rocks (conglomerate, sandstone, mudstone), volcanic rocks (andesite, basalt and pyroclastics) and granitic rocks which cut them are Eocene. The Miocene units are composed of clastic sedimentary rocks interbedded with tephrite, basalt and pyroclastics. Pliocene clastic deposits consisting of conglomerate, sandstone, siltstone and marl alternation (Figure 1).

The primary porosity of the volcanic rocks, generally composed of basalts of the Late Cretaceous, is very low in SGF and its surround. The fractured structures, which they have because of tectonic activities, provide secondary porosity to the rocks and permeability in places. These non-homogeneous permeable levels throughout the units allow the surface waters to flow deeper along the faults. In the areas, where slant topography is dominant, the waters flowing to shallow depths emerge from the slopes in the form of low discharge springs. Therefore, the volcanic rocks are important in fractured grounds in terms of groundwater.

The units consisting of clastic rocks like conglomerate, sandstone and siltstone of the Jurassic age in and around İGF are permeable. The Late

Cretaceous and Eocene units, which are generally volcano-sedimentary in character, are permeable in areas where pyroclastic rocks represented by agglomerate and tuff outcrops. The permeability of rocks such as granite and granodiorite, which form the granitoid widely exposed in the study area, are very low in non-fractured and unweathered areas. However, the three directional fracture systems developed in these rocks gave the granitoid a permeable property. In addition, the bonds between the minerals have become weak and the rocks have dispersed on the surface and shallow depths in the rocks where different degrees of weathering are observed. Therefore, the granitoid is permeable in areas where it is fractured and weathered, and impermeable in unfractured and unweathered areas.

The units of Late Cretaceous basaltic and andesitic rocks have not permeability in AGF, but the pyroclastics outcropping in the form of tuffs are permeable. The well-developed fracture systems of the granitoid outcropping in a large area have provided permeability to the unit. The spring waters discharging from cracks every season prove this.

The clastic sedimentary and volcanic rocks generally crop out in ŞGF. The fact that the rocks such as; conglomerate, sandstone and siltstone of which their primary porosities are high permeable, show variation according to their degree of cementation.
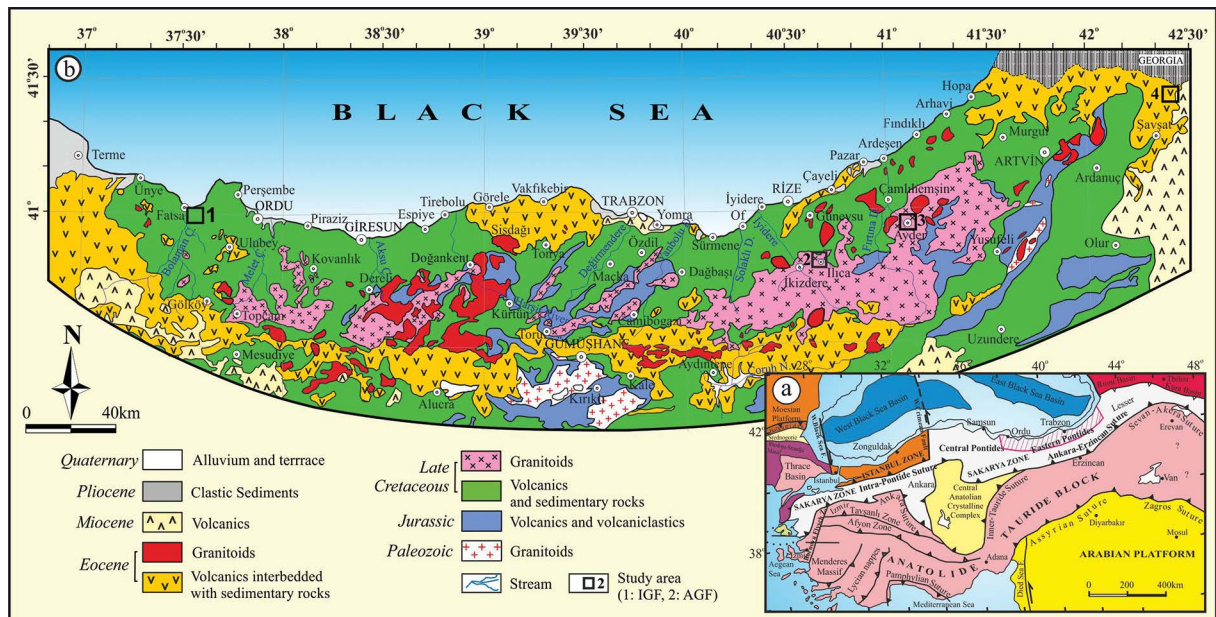


Figure 1- a) The tectonic map of Turkey (modified from Okay and Tüysüz, 1999), b) distribution of volcanic and intrusive rocks in East Pontides (modified from Güven, 1993; Arslan et al., 2013; Yücel, 2013 and Temizel et al., 2016).

The primary porosities of the volcanic rocks are low, but their improved structures and tectonic activities during cooling provided them to be in fractured. The tuffs of the Late Cretaceous units in the area are permeable, and volcanic rocks such as dacite and rhyodacite are impermeable.

## 4. Major Ions

In order to determine the chemical properties of the waters in the investigated areas, the samples were taken from the geothermal wells, hot and cold springs and surface waters. In SGF, the sampling and in-situ measurements were made from hot spring (SARKAP), two cold springs (SSK, QK), and the surface water draining the basin (IDD-IDB). The sampling and measurement studies in İGF were made from the geothermal well (ILKAP), one from the cold spring (ISK) and from the surface water near the geothermal drilling (IDERY-IDERA). In AGF, one sample from the geothermal well (AYKAP), two samples from hot springs (AYKÖPK, AYESH), one from cold spring (HOŞSU) and from the surface water (AYDEREY-AYDEREA) were taken and measured.

The in-situ measurement and sampling was carried out from geothermal wells (ILICAS), mineral water (CDMS), cold spring (SKSK) and from the surface water (CERDERY-CERDEA). The descriptions, coordinates and elevation values of the sample points taken are given in table 1.

The hot spring (SARKAP) in SGF has the temperature of 47°C, EC of 1935 µs/cm and pH value of 8.05 from in situ measurements. Mg ions are quite low values (Table 2) in dominant anion and cations of the Na and $SO_4$ ions in the hot spring. The temperatures of two different cold springs (SSK and ÇK) in this area is approximately 14°C and EC values are 174 and 337 µS/cm, respectively. Ca and $HCO_3$ ions are dominant in cold springs with pH values of about 7. The surface waters (IDD-IDB) in the field has a pH of about 8 and EC of 84-94 µS/cm and Ca and $HCO_3$ ions are dominant in these waters.

60°C temperature and 7.03 pH value were measured in the geothermal well in IGF. Dominated anions and cations in the hot spring are Na and $HCO_3$ ions with EC of 6633 µS/cm (Table 2). Ca and $HCO_3$ ions are dominant in the cold spring in IGF with a pH

Table 1- Sampling coordinates in the study area.

| | Sample No | Coordinate (UTM 37 T WGS84) | Elevation (m) |
|---|---|---|---|
| Sarmaşık (Ordu) Geothermal Field | SARKAP (Hot spring) | 0383154 - 4536830 | 102 |
| | SSK (Cold spring) | 0383064 - 4536784 | 101 |
| | ÇK (Cold spring) | 0375853 - 4532828 | 225 |
| | IDD (Surface water) | 0383619 - 4536877 | 100 |
| | IDB (Surface water) | 0383071 - 4536795 | 104 |
| İkizdere (Rize) Geothermal Field | ILKAP (Geothermal well) | 0635840 - 4515969 | 848 |
| | ISK (Cold spring) | 0637838 - 4516474 | 995 |
| | IDERY (Surface water) | 0636570 - 4516090 | 966 |
| | IDERA (Surface water) | 0635555 - 4516034 | 821 |
| Ayder (Rize) Geothermal Field | AYKAP (Geothermal well) | 0676703 - 4535711 | 1228 |
| | AYKÖPK (Hot spring) | 0673100 - 4541100 | 825 |
| | AYESH (Hot spring) | 0676356 - 4535638 | 1200 |
| | HOŞSU (Cold spring) | 0677192 - 4535639 | 1271 |
| | AYDEREA (Surface water) | 0673500 - 4539500 | 1050 |
| | AYDEREY (Surface water) | 0678212 - 4535863 | 1300 |
| Şavşat (Artvin) Geothermal Field | ILICAS (Geothermal well) | 0282740 - 4586153 | 1495 |
| | CDMS (Mineral spring) | 0281351 - 4573470 | 1145 |
| | ŞSSK (Cold spring) | 0282628 - 4588250 | 1550 |
| | CERDERY (Surface water) | 0282940 - 4585958 | 1496 |
| | CERDERA (Surface water) | 0281280 - 4586418 | 1490 |

Table 2- Physicochemical parameters of the analyzed waters.

| Sample No | Temperature (°C) | pH | EC (µS/cm) | TDS mg/L | Ca mg/L | Mg mg/L | Na mg/L | K mg/L | Cl mg/L | Alkalinity ($HCO_3+CO_3$) mg/L | $SO_4$ mg/L | % Error |
|---|---|---|---|---|---|---|---|---|---|---|---|---|
| **Sarmaşık Geothermal Field** | | | | | | | | | | | | |
| SARKAP | 47 | 8.05 | 1935 | 1260 | 213.13 | 0.33 | 261.90 | 3.79 | 97.12 | 11.76 | 875.8 | 1.43 |
| SSK | 14.5 | 7.8 | 174 | 141 | 51.86 | 7.55 | 14.06 | 3.39 | 2.35 | 203.33 | 5.24 | 2.90 |
| CK | 14 | 7.08 | 337 | 272 | 112.23 | 7.18 | 15.02 | 3.86 | 5.27 | 370.78 | 8.49 | 1.95 |
| IDD | 15.2 | 8.27 | 94 | 69 | 25.82 | 4.34 | 6.69 | 0.66 | 2.15 | 101.66 | 3.66 | 0.47 |
| IDB | 15.8 | 7.87 | 84 | 66 | 23.29 | 3.76 | 5.37 | 0.54 | 1.52 | 89.70 | 3.42 | 0.62 |
| **İkizdere Geothermal Field** | | | | | | | | | | | | |
| ILKAP | 60 | 7.03 | 6633 | 2587 | 331.31 | 79.01 | 965.65 | 140.66 | 464.12 | 2810 | 296.2 | 3.03 |
| ISK | 11.8 | 7.34 | 22 | 19 | 7.24 | 0.71 | 3.09 | 0.40 | 0.30 | 23.92 | 1.49 | 2.98 |
| IDERY | 9.1 | 6.4 | 17 | 16 | 6.82 | 0.72 | 1.32 | 0.37 | 0.14 | 23.92 | 2.38 | 2.46 |
| IDERA | 9.2 | 7.4 | 19 | 17 | 7.08 | 0.80 | 1.71 | 0.53 | 0.38 | 23.92 | 2.49 | 4.76 |
| **Ayder Geothermal Field** | | | | | | | | | | | | |
| AYKAP | 55 | 9.15 | 233 | 97 | 8.74 | 0.06 | 39.93 | 0.73 | 2.69 | 35.3 | 38.1 | 2.97 |
| AYKOPK | 31.7 | 9.32 | 296 | 171 | 16.77 | 0.26 | 63.66 | 1.06 | 9.77 | 24 | 118 | 0.93 |
| AYESH | 20 | 8.16 | 33 | 24 | 8.26 | 1.24 | 12.8 | 0.36 | 1.36 | 30.5 | 12.5 | 4.29 |
| HOSSU | 10.8 | 7.56 | 35 | 31 | 9.25 | 1.73 | 3.83 | 0.89 | 0.48 | 36.6 | 1.51 | 3.91 |
| AYDEREA | 7.7 | 6.84 | 22 | 21 | 5.19 | 0.5 | 1.21 | 0.31 | 0.13 | 18.3 | 1.96 | 1.42 |
| AYDEREY | 10.3 | 7.3 | 19 | 17 | 7.49 | 1.03 | 2.07 | 0.61 | 0.10 | 0.49 | 1.62 | 3.34 |
| **Savşat Geothermal Field** | | | | | | | | | | | | |
| ILICAS | 39 | 6.9 | 5734 | 3044 | 288 | 46.35 | 1323 | 35.14 | 1052 | 2601 | 166 | 0.90 |
| SSSK | 9.2 | 7.59 | 155 | 144 | 55.75 | 8.07 | 11.46 | 0.08 | 1.25 | 191.37 | 4.79 | 1.81 |
| CDMS | 12 | 6.2 | 2741 | 2369 | 369.4 | 60.07 | 1003 | 22.28 | 771.89 | 2379 | 150 | 2.89 |
| CERDERA | 13.8 | 8.53 | 411 | 340 | 50.9 | 9.07 | 116.46 | 2.91 | 83.69 | 251.18 | 17.6 | 4.45 |
| CERDERY | 8.6 | 7.92 | 122 | 116 | 43.15 | 6.55 | 13.4 | 0.42 | 1.13 | 155.49 | 4.9 | 4.26 |

value of 7.34, an EC of 22 μS/cm (Table 2). Ca and $HCO_3$ ions are dominant in the surface water draining the basin with a pH value of 6.7 and EC value of 18 μS/cm.

During the in-situ measurements in AGF, where Na, $CO_3$ and $SO_4$ ions are dominant, the temperature of the geothermal well is 55°C, the pH value is 9.15 and EC value is 233 μS/cm (Table 2). Looking at two naturally hot springs discharging in this field, AYESH has a temperature of 20°C, pH value of 8.16 and EC value of 33 μS/cm. The other hot spring, AYKÖPK, has the temperature of 30°C, pH of 9.32 and EC of 266 μS/cm. In AYESH, Na and $HCO_3$ ions are dominant, whereas in AYKÖPK, Na and $SO_4$ ions are dominant (Table 2). The cold spring (HOŞSU) in the field has dominant Ca and $HCO_3$ ions with a pH value of 7.56 and an EC of 35 μS/cm. The pH of the surface water in the field is around 7, and the EC value is 19 μS/cm in upper elevations and 22 μS/cm in lower elevations and the dominant anions and cations are Ca and $HCO_3$.

The geothermal well water (ILICAS) has a temperature of 39°C, a pH value of 6.9 an EC of 5734

μS/cm in ŞGF. Na and $HCO_3$ ions are dominant in the well water. The pH of the mineral water (CDMS) is 6.2, the EC value is 2741 μS/cm and the dominant anions and cations are Na and $HCO_3$. The pH and EC values of the cold spring (ŞSSK), which is dominant in Ca and $HCO_3$ ions, are 7.59 and 155 μS/cm, respectively. The chemical properties of the river water are different from each other before (CERDERY) and after (CERDERA) the mixing of the hot spring (Table 2). CERDERY has a pH of 7.92, an EC value of 122 μS/cm with dominant anions and cations are Ca and $HCO_3$. However, CERDERA has the EC value of 411 μS/cm with dominant anions and cations of Na and $HCO_3$. The drill water flowing out has physically and chemically influenced the river water that runs nearby.

When the plots of waters in the Piper Diagram for the geothermal fields of the Eastern Black Sea Region are evaluated, the earth alkaline elements in the hot waters (Ca+Mg) in the SGF and strong acid (Cl + $SO_4$) roots are higher than alkaline elements (Na+K) and weak acid roots ($CO_3$ + $HCO_3$), respectively. However, the opposite situation is observed in cold spring and surface waters (Figure 2). In IGF, AGF and ŞGF hot
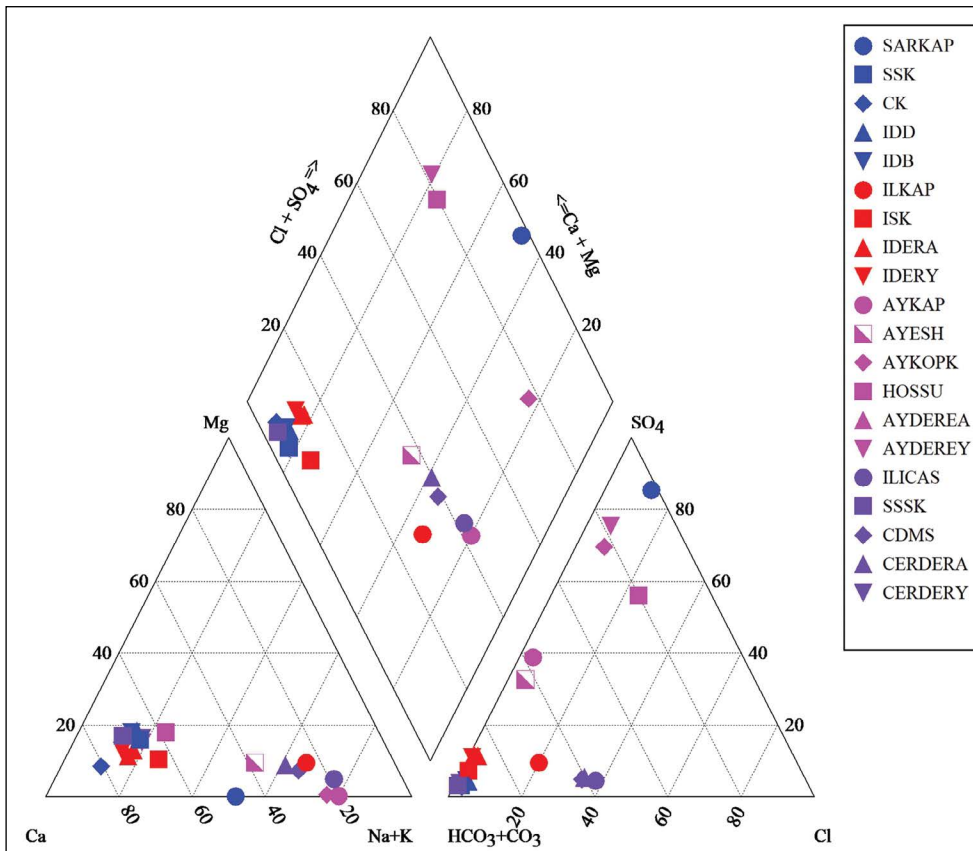


Figure 2- Piper diagrams of the investigeted water samples

springs, the alkaline elements (Na+K) and weak acid roots (CO$_3$+HCO$_3$) are more than the earth alkaline elements (Ca+Mg) and strong acid (Cl+SO$_4$) roots. CO$_3$ and SO$_4$ values in the Ayder hot springs with very low Cl content, are approximately the same, however; Cl and HCO$_3$ ions in the Şavşat hot springs with low SO$_4$ are in the same values. In all three areas, the earth alkaline elements (Ca + Mg) and weak acid roots (CO$_3$ + HCO$_3$) in cold springs and surface waters are more than the alkaline elements (Na + K) and strong acid (Cl + SO$_4$) roots respectively (Figure 2).

The saturation indices for different minerals were calculated by using thermodynamic modeling to estimate the degree of interaction of the waters in the study area with host rocks (Table 3). The primary minerals, which are determined microscopically in volcanic rocks that are exposed in geothermal fields, are silicate minerals like; plagioclase, alkaline feldspar, augite, hornblende and quartz, and the secondary minerals are; calcite, quartz and chlorite. The sedimentary rocks in the surrounding are formed by the lacustrine deposits which the limestone, sandstone, marl, cherty limestone and gypsum lenses are observed. The saturation index (SI) values belonging to the selected minerals considering these lithologies were calculated using the pH and chemical analysis results in the field utilizing the PHREEQC software included in the AquaChem 2014.1 software (Table 3).

When the SI values are examined, hot and cold waters in the studied areas are not saturated with sulphate minerals such as anhydrite and gypsum. Sarmaşık hot and cold springs show a tendency for slight oversaturation to dolomite and calcite, but unsaturated with dolomite. The surface waters are approximately in equilibrium state with calcite (Figure 3a). İkizdere geothermal well water is saturated with aragonite, calcite, barite and dolomite minerals. Cold spring and surface waters are not saturated with any of the selected minerals (Figure 3b). While the Ayder hot geothermal well water is slightly saturated with aragonite, calcite and dolomite, the cold spring and surface waters are unsaturated (Figure 3c). Şavşat geothermal water and Ciritdüzü mineral water are saturated with aragonite, calcite and dolomite, however; the surface waters are not saturated (Figure 3d). While the hot springs of İkizdere and Şavşat are saturated with K-feldspar representatively selected for

silicate minerals, the Sarmaşık and Ayder hot springs are not saturated. All hot and cold springs except the Ayder hot spring are saturated with K-mica mineral. All hot and cold waters except for the hot springs of Ayder are saturated with clay minerals such as; kaolinite and illite. All warm waters except the Şavşat hot springs are saturated with talc mineral. All hot waters except the Ayder geothermal well water shows a slight tendency to oversaturation to quartz mineral, whereas the Ayder geothermal well water show a slight tendency towards sub-saturation. All hot and cold waters show a super saturation to minerals such as goethite and hematite (Table 3).

## 5- Rare Earth Elements (REEs) and Yttrium

Although their positions in the periodic table are close to each other, the REE+Y have different physicochemical properties and are widely used in the interpretation of geochemical processes in water-rock interaction. In addition, these elements may reflect changes in response to anthropogenic or natural anomaly effects in hydrogeological environments (Bragin et al., 2018).

REE+Y concentrations of the waters analyzed in the studied geothermal fields and their close vicinities and the exposed samples collected are shown in table 4. REE+Y distribution models normalized to chondrite (Sun and McDonough, 1989) are given in figure 4. When the figures 4b, d, f and h are examined, REE+Y patterns in the waters in all areas are almost similar to each other except for the minor differences. This situation shows that the host rocks in which the water is circulating are of similar type.

When the table 4 and figure 4 are evaluated, the ∑REE concentrations in the analyzed waters are 0.06-1.83 ppb in SGF, 0.64-2.13 ppb in IGF, 0.01-0.3 ppb in AGF, and 0.03-2.13 ppb in SGF. The highest ∑REE concentration in geothermal waters was measured in ILKAP (İkizdere) and ILICAS (Şavşat) (∑REE = 2.13 ppb) samples. The lowest REE concentrations (∑REE = 0.01-0.3 ppb) were measured in AGF waters with the highest pH value (8.60-9.86), and the lowest TDS value (52-173 mg/L).

The chondrite normalized La$_{CN}$/Gd$_{CN}$ ratios are higher than 1 (except CERDERA and IDD) and Yb$_{CN}$/Gd$_{CN}$ ratios (excluding ILICAS) are less than 1 in all

Table 3- Saturation index calculations for some minerals in the analyzed waters.

| Minerals | Formula | Sarmaşık Geothermal Field | | | | İkizdere Geothermal Field | | |
|---|---|---|---|---|---|---|---|---|
| | | SARKAP | SSK | CK | IDD | ILKAP | ISK | IDERY |
| Albite | $NaAlSi_3O_8$ | -0.85 | -0.98 | -2.33 | -1.40 | 0.49 | -2.71 | -4.40 |
| Anhydrite | $CaSO_4$ | -0.63 | -3.15 | -2.72 | -3.52 | -1.06 | -4.33 | -4.15 |
| Aragonite | $CaCO_3$ | 0.38 | 0.09 | -0.09 | 0.01 | 1.43 | -1.36 | -3.09 |
| Barite | $BaSO_4$ | 1.09 | -1.76 | -0.56 | -1.85 | 0.43 | -1.34 | -1.59 |
| Ca-Montmorillonite | $Ca0.165Al_2.33Si_3.67O_{10}(OH)_2$ | -0.75 | 4.33 | 3.58 | 3.41 | 3.40 | 3.54 | 3.79 |
| Calcite | $CaCO_3$ | 0.51 | 0.24 | 0.06 | 0.16 | 1.55 | -1.93 | -2.93 |
| Celestine | $SrSO_4$ | -0.86 | -3.53 | -2.52 | -3.99 | -1.1 | -4.9 | -4.82 |
| Dolomite | $CaMg(CO_3)_2$ | -1.36 | -0.15 | -0.89 | -0.24 | 2.99 | -4.71 | -6.73 |
| Flourite | $CaF_2$ | -0.13 | -2.77 | -2.86 | -3.57 | -1.22 | -3.70 | -5.04 |
| Gypsum | $CaSO_4{:}2H_2O$ | -0.54 | -2.90 | -2.47 | -3.27 | -1.08 | -4.08 | -3.90 |
| Goethite | $FeOOH$ | 7.57 | 8.07 | 7.01 | 7.91 | 7.91 | 6.60 | 3.77 |
| Halite | $NaCl$ | -6.29 | -9.01 | -8.66 | -9.36 | -5.13 | -10.51 | -11.21 |
| Illite | $K0.6Mg0.25Al_2.3Si_3.5O_{10}(OH)_2$ | -0.74 | 3.62 | 2.32 | 2.67 | 3.35 | 1.86 | 1.40 |
| K-Feldsar | $KAlSi_3O_8$ | -0.61 | 0.88 | -0.44 | 0.06 | 1.61 | -1.08 | -2.40 |
| K-Mica | $KAl_3Si_3O_{10}(OH)_2$ | 4.55 | 10.02 | 9.13 | 8.65 | 9.67 | 8.49 | 8.94 |
| Kaolinite | $Al_2Si_2O_5(OH)_4$ | 0.59 | 5.36 | 5.22 | 4.59 | 4.17 | 5.57 | 6.26 |
| Quartz | $SiO_2$ | 0.13 | 0.49 | 0.21 | 0.39 | 0.49 | 0.24 | -0.16 |
| Rhodochrosite | $MnCO_3$ | -1.63 | -3.14 | - | - | -0.06 | - | -4.56 |
| Siderite | $FeCO_3$ | -6.70 | -0.99 | -0.34 | -2.43 | -0.52 | -2.32 | -3.16 |
| Talc | $Mg_3Si_4O_{10}(OH)_2$ | 4.50 | -1.38 | -7.12 | 0.54 | 3.14 | -8.49 | - |
| Viterite | $BaCO_3$ | -3.00 | -4.01 | -3.43 | -3.81 | -1.99 | -4.60 | -6.08 |

Table 3- (continue)

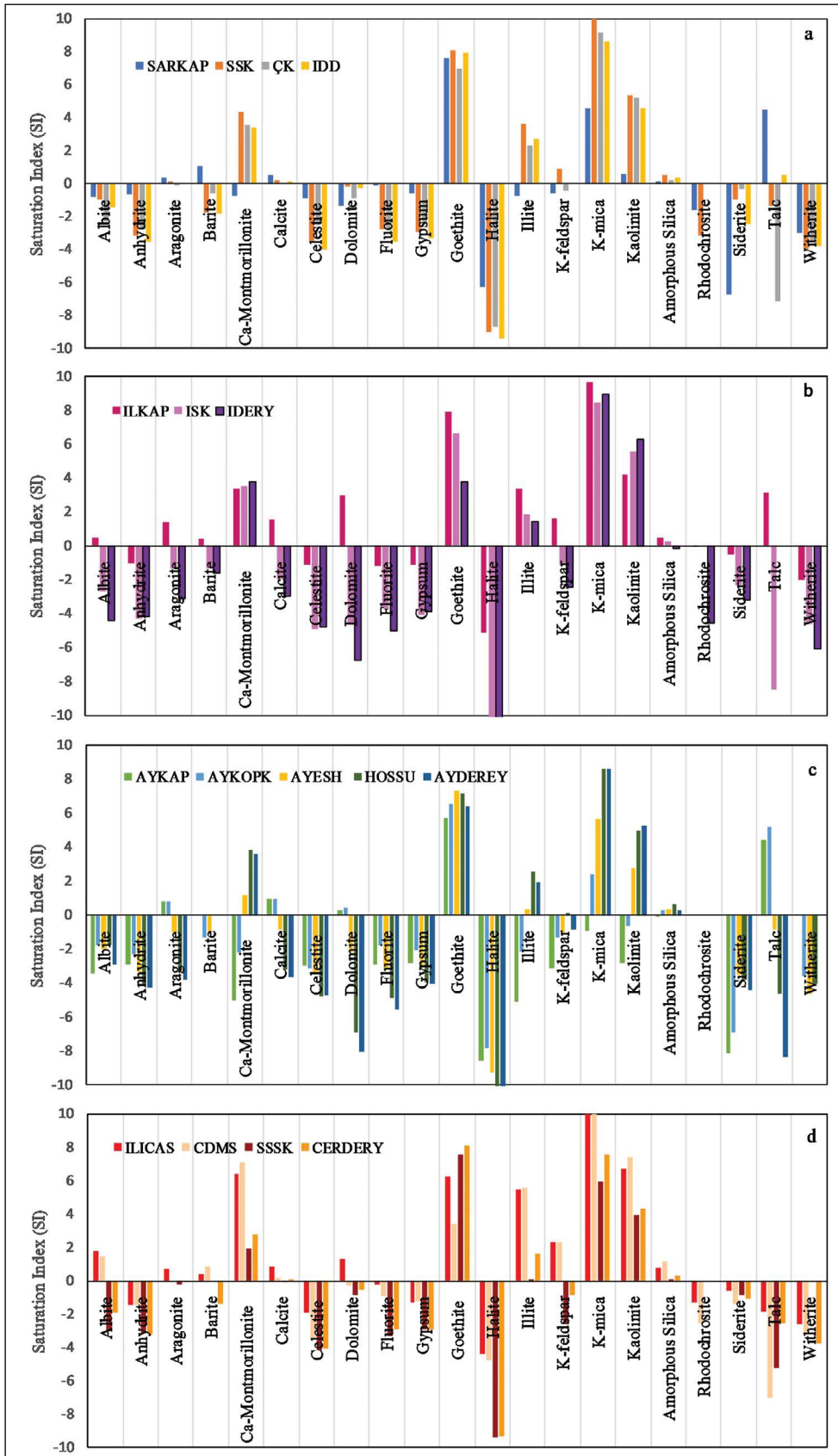| Minerals | Formula | Ayder Geothermal Field | | | | | Savşat Geothermal Field | | | |
|---|---|---|---|---|---|---|---|---|---|---|
| | | AYKAP | AYKOPK | AYESH | HOSSU | AYDEREY | ILICAS | CDMS | SSSK | CERDERY |
| Albite | $NaAlSi_3O_8$ | -3.42 | -1.79 | -1.99 | -1.79 | -2.89 | 1.75 | 1.48 | -3.01 | -1.90 |
| Anhydrite | $CaSO_4$ | -2.88 | -2.30 | -3.39 | -4.22 | -4.27 | -1.47 | -1.47 | -3.15 | -3.22 |
| Aragonite | $CaCO_3$ | 0.81 | 0.78 | -1.01 | -3.32 | -3.82 | 0.69 | 0.00 | -0.20 | -0.07 |
| Barite | $BaSO_4$ | - | -1.30 | -1.01 | - | - | 0.41 | 0.82 | - | -1.41 |
| Ca-Montmorillonite | $Ca0.165Al_{3}.33Si_3.67O_{10}(OH)_2$ | -5.05 | -2.22 | 1.20 | 3.79 | 3.56 | 6.40 | 7.10 | 1.91 | 2.78 |
| Calcite | $CaCO_3$ | 0.94 | 0.92 | -0.86 | -3.17 | -3.66 | 0.83 | 0.16 | -0.04 | 0.09 |
| Celestine | $SrSO_4$ | -2.99 | -3.16 | -3.45 | -4.76 | -4.70 | -1.94 | -3.49 | -4.17 | -4.07 |
| Dolomite | $CaMg(CO_3)_2$ | 0.28 | 0.45 | -2.26 | -6.93 | -8.05 | 1.28 | -0.32 | -0.82 | -0.54 |
| Flourite | $CaF_2$ | -2.94 | -1.77 | -3.24 | -4.89 | -5.56 | -0.23 | -0.94 | -3.27 | -2.91 |
| Gypsum | $CaSO_4:2H_2O$ | -2.85 | -2.11 | -3.16 | -3.97 | -4.01 | -1.33 | -1.21 | -2.90 | -2.96 |
| Goethite | $FeOOH$ | 5.71 | 6.51 | 7.32 | 7.18 | 6.40 | 6.24 | 3.38 | 7.54 | 8.10 |
| Halite | $NaCl$ | -8.59 | -7.79 | -9.28 | -10.22 | -11.12 | -4.40 | -4.77 | -9.37 | -9.33 |
| Illite | $K0.6Mg0.25Al_2.3Si_3.5O_{10}(OH)_2$ | -5.11 | -2.14 | 0.31 | 2.51 | 1.97 | 5.49 | 5.54 | 0.12 | 1.63 |
| K-Feldsar | $KAlSi_3O_8$ | -3.14 | -1.30 | -1.14 | 0.09 | -0.89 | 2.31 | 2.33 | -2.62 | -0.85 |
| K-Mica | $KAl_3Si_3O_{10}(OH)_2$ | -0.93 | 2.36 | 5.66 | 8.58 | 8.60 | 12.28 | 12.20 | 5.95 | 7.54 |
| Kaolinite | $Al_2Si_2O_5(OH)_4$ | -2.80 | -0.60 | 2.79 | 4.98 | 5.27 | 6.72 | 7.41 | 3.93 | 4.30 |
| Quartz | $SiO_2$ | -0.08 | 0.26 | 0.38 | 0.63 | 0.28 | 0.78 | 1.15 | 0.07 | 0.34 |
| Rhodochrosite | $MnCO_3$ | - | - | - | - | - | -1.32 | -2.51 | - | - |
| Siderite | $FeCO_3$ | -8.12 | -6.90 | -3.54 | -3.85 | -4.40 | -0.60 | -1.37 | -0.88 | -1.04 |
| Talc | $Mg_3Si_4O_{10}(OH)_2$ | 4.43 | 5.16 | -0.83 | -4.63 | -8.33 | -1.84 | -7.00 | -5.26 | -2.55 |
| Viterite | $BaCO_3$ | - | -3.56 | -4.61 | -4.06 | - | -2.63 | -3.23 | - | -3.80 |

Figure 3- Saturation indices of some selected minerals a) Sarmaşık geothermal field, b) İkizdere geothermal field c) Ayder geothermal field, d) Şavşat geothermal field.

Table 4- REE+Yttrium concentrations of the analyzed waters (rocks:ppm, waters:ppb, bdl: below detection limit).

| | | La | Ce | Pr | Nd | Sm | Eu | Gd | Tb | Dy | Y | Ho | Er | Tm | Yb | Lu |
|---|---|---|---|---|---|---|---|---|---|---|---|---|---|---|---|---|
| **SARMAŞIK GEOTHERMAL FIELD (SGF)** | | | | | | | | | | | | | | | | |
| F-3 | Tuffite | 7.9 | 12.6 | 1.64 | 6.8 | 1.47 | 0.48 | 1.55 | 0.24 | 1.56 | 7.9 | 0.26 | 0.94 | 0.11 | 0.75 | 0.12 |
| F-5 | Sandy Lst. | 4 | 6.1 | 0.8 | 3.2 | 0.59 | 0.14 | 0.64 | 0.09 | 0.54 | 3.9 | 0.13 | 0.36 | 0.06 | 0.36 | 0.05 |
| F-8 | Basaltic tuff | 16 | 34.2 | 4.5 | 20.1 | 4.43 | 1.42 | 4.77 | 0.75 | 4.56 | 24.6 | 0.95 | 2.67 | 0.4 | 2.47 | 0.4 |
| F-10 | Basalt | 29.6 | 51.3 | 5.26 | 17.5 | 3.21 | 0.57 | 2.86 | 0.47 | 2.83 | 18.7 | 0.61 | 2.07 | 0.33 | 2.24 | 0.39 |
| SARKAP | Hot spring | 0.129 | 0.486 | 0.058 | 0.773 | 0.054 | 0.224 | 0.02 | 0.007 | 0.015 | 0.17 | 0.007 | 0.018 | 0.002 | 0.017 | 0.023 |
| SSK | Cold spring | bdl | bdl | 0.004 | 0.025 | 0.008 | 0.005 | 0.006 | 0.001 | 0.006 | 0.044 | 0.001 | 0.004 | 0 | 0.003 | 0.001 |
| ÇK- | Cold spring | bdl | bdl | bdl | 0.016 | 0.023 | 0.044 | bdl | 0.001 | bdl | 0.085 | bdl | 0.002 | bdl | 0.002 | bdl |
| IDD | Surface water | 0.013 | 0.074 | 0.01 | 0.043 | 0.012 | 0.005 | 0.017 | 0.002 | 0.013 | 0.069 | 0.001 | 0.009 | 0.001 | 0.004 | 0.001 |
| IDB | Surface water | 0.023 | 0.065 | 0.017 | 0.06 | 0.014 | 0.005 | 0.015 | 0.002 | 0.012 | 0.083 | 0.002 | 0.01 | 0 | 0.008 | 0.001 |
| **İKİZDERE GEOTHERMAL FIELD (IGF)** | | | | | | | | | | | | | | | | |
| IK-1 | Granite | 31.6 | 57.2 | 6.06 | 20.6 | 3.6 | 0.75 | 3.66 | 0.58 | 3.74 | 22.2 | 0.77 | 2.36 | 0.38 | 2.57 | 0.4 |
| IK-2 | Granite | 15.2 | 27.8 | 3.09 | 11.4 | 2.36 | 0.5 | 2.63 | 0.43 | 2.99 | 18.3 | 0.64 | 2.08 | 0.31 | 2.14 | 0.36 |
| ILKAP | Geothermal well | 0.126 | 0.61 | 0.054 | 0.762 | 0.089 | 0.286 | 0.043 | 0.01 | 0.039 | 0.432 | 0.005 | 0.039 | 0.005 | 0.032 | 0.027 |
| ISK | Cold spring | 0.155 | 0.273 | 0.046 | 0.17 | 0.039 | 0.017 | 0.039 | 0.004 | 0.027 | 0.183 | 0.003 | 0.022 | 0.003 | 0.018 | 0.003 |
| IDERA | Surface water | 0.1 | 0.217 | 0.039 | 0.141 | 0.035 | 0.009 | 0.027 | 0.004 | 0.03 | 0.18 | 0.004 | 0.016 | 0.002 | 0.015 | 0.004 |
| IDERY | Surface water | 0.083 | 0.316 | 0.033 | 0.113 | 0.023 | 0.01 | 0.019 | 0.004 | 0.022 | 0.157 | 0.003 | 0.014 | 0.002 | 0.012 | 0.004 |
| **AYDER GEOTHERMAL FIELD (AGF)** | | | | | | | | | | | | | | | | |
| AY-1 | Granodiorite | 0.9 | 2.6 | 0.52 | 3 | 1.21 | 0.92 | 1.84 | 0.34 | 2.3 | 12.4 | 0.49 | 1.53 | 0.21 | 1.35 | 0.2 |
| AY-2 | Granodiorite | 30.4 | 45.9 | 4.66 | 15 | 2.18 | 0.6 | 1.62 | 0.22 | 1.31 | 7.1 | 0.25 | 0.74 | 0.11 | 0.8 | 0.13 |
| AY-3 | Basalt | 17.5 | 36.7 | 4.97 | 21 | 5.04 | 1.44 | 6.16 | 1.1 | 7.17 | 42.5 | 1.62 | 4.99 | 0.74 | 5.1 | 0.81 |
| AYKAP | Geothermal well | bdl | bdl | 0.003 | bdl | 0.003 | 0.002 | bdl | 0 | 0.0035 | 0.004 | 0 | 0.003 | 0 | 0 | 0.001 |
| AYESH | Hot spring | bdl | bdl | bdl | bdl | 0.001 | 0.004 | bdl | 0 | 0 | 0.004 | 0 | 0.001 | 0 | 0 | bdl |
| AYKOPK | Hot spring | bdl | bdl | 0.002 | 0.011 | 0.002 | 0.002 | 0.002 | 0.001 | 0.009 | 0.01 | 0 | 0.003 | 0 | 0.0035 | 0 |
| HOSSU | Cold spring | bdl | bdl | 0.003 | 0.006 | 0.0015 | 0.001 | bdl | 0.0005 | 0.003 | 0.003 | 0 | 0.002 | 0 | 0 | 0.001 |
| AYDEREY | Surface water | 0.028 | 0.091 | 0.005 | 0.0116 | 0.004 | 0.0035 | 0.014 | 0.001 | 0.002 | 0.0193 | bdl | 0.0013 | 0 | 0.0025 | 0.0005 |
| AYDEREA | Surface water | 0.077 | 0.122 | 0.0115 | 0.0525 | 0.009 | 0.006 | 0.0095 | 0.001 | 0.0105 | 0.0535 | 0 | 0.0105 | 0 | 0.0075 | 0.002 |

Table 4- (continue)

| | | La | Ce | Pr | Nd | Sm | Eu | Gd | Tb | Dy | Y | Ho | Er | Tm | Yb | Lu |
|---|---|---|---|---|---|---|---|---|---|---|---|---|---|---|---|---|
| | | | | | | | ŞAVŞAT GEOTHERMAL FIELD (SGF) | | | | | | | | | |
| SV-1 | Sandstone | 5.4 | 11.2 | 1.56 | 7.1 | 2.07 | 0.72 | 2.28 | 0.38 | 2.45 | 13.6 | 0.52 | 1.53 | 0.23 | 1.45 | 0.22 |
| SV-2 | Sandstone | 8.8 | 17.8 | 2.47 | 10.7 | 2.96 | 0.89 | 3.19 | 0.54 | 3.24 | 18.2 | 0.73 | 2.02 | 0.3 | 1.88 | 0.3 |
| TD-1 | Trachyandesitet | 16.1 | 29.2 | 3.13 | 11.2 | 1.86 | 0.53 | 1.17 | 0.13 | 0.65 | 3 | 0.11 | 0.27 | 0.03 | 0.25 | 0.03 |
| TD-3 | Trachyandesitet | 14.9 | 25.5 | 2.73 | 9.5 | 1.52 | 0.53 | 0.92 | 0.11 | 0.5 | 2.4 | 0.1 | 0.18 | 0.03 | 0.19 | 0.03 |
| C-1 | Volcanogenic sst. | 4.4 | 9.1 | 1.3 | 6.4 | 1.77 | 0.71 | 2.17 | 0.36 | 2.43 | 12.9 | 0.5 | 1.5 | 0.2 | 1.33 | 0.2 |
| C-7 | Volcanogenic sst. | 5.3 | 11.1 | 1.54 | 7.2 | 1.9 | 0.72 | 2.38 | 0.38 | 2.38 | 13.9 | 0.53 | 1.57 | 0.21 | 1.42 | 0.22 |
| TRV-1 | Travertine | 2.5 | 3.5 | 0.53 | 2 | 0.55 | 0.2 | 0.93 | 0.18 | 1.3 | 13.2 | 0.29 | 0.92 | 0.12 | 0.85 | 0.13 |
| ILICAS | Geothermal well | 0.358 | 0.593 | 0.051 | 0.649 | 0.047 | 0.272 | 0.027 | 0.004 | 0.042 | 0.396 | 0.004 | 0.029 | 0.002 | 0.033 | 0.024 |
| CDMS | Mineral spring | 0.18 | 0.615 | 0.0575 | 0.8075 | 0.038 | 0.1955 | 0.0585 | 0.0075 | 0.043 | 0.301 | 0.002 | 0.0285 | 0.0025 | 0.016 | 0.003 |
| ŞSSK | Cold spring | öla | öla | 0.003 | 0.016 | 0.0025 | 0.0015 | 0.002 | 0.001 | 0 | 0.0103 | 0 | 0.002 | 0 | 0.002 | 0.0015 |
| CERDERA | Surface water | 0.005 | 0.02 | 0.038 | 0.138 | 0.021 | 0.118 | 0.0285 | 0.002 | 0.0225 | 0.124 | 0.005 | 0.0055 | 0.001 | 0.013 | 0.028 |
| CERDERY | Surface water | 0.068 | 0.27 | 0.02 | 0.039 | 0.013 | 0.005 | 0.014 | 0.002 | 0.013 | 0.12 | 0.002 | 0.008 | 0.001 | 0.006 | 0.004 |

146
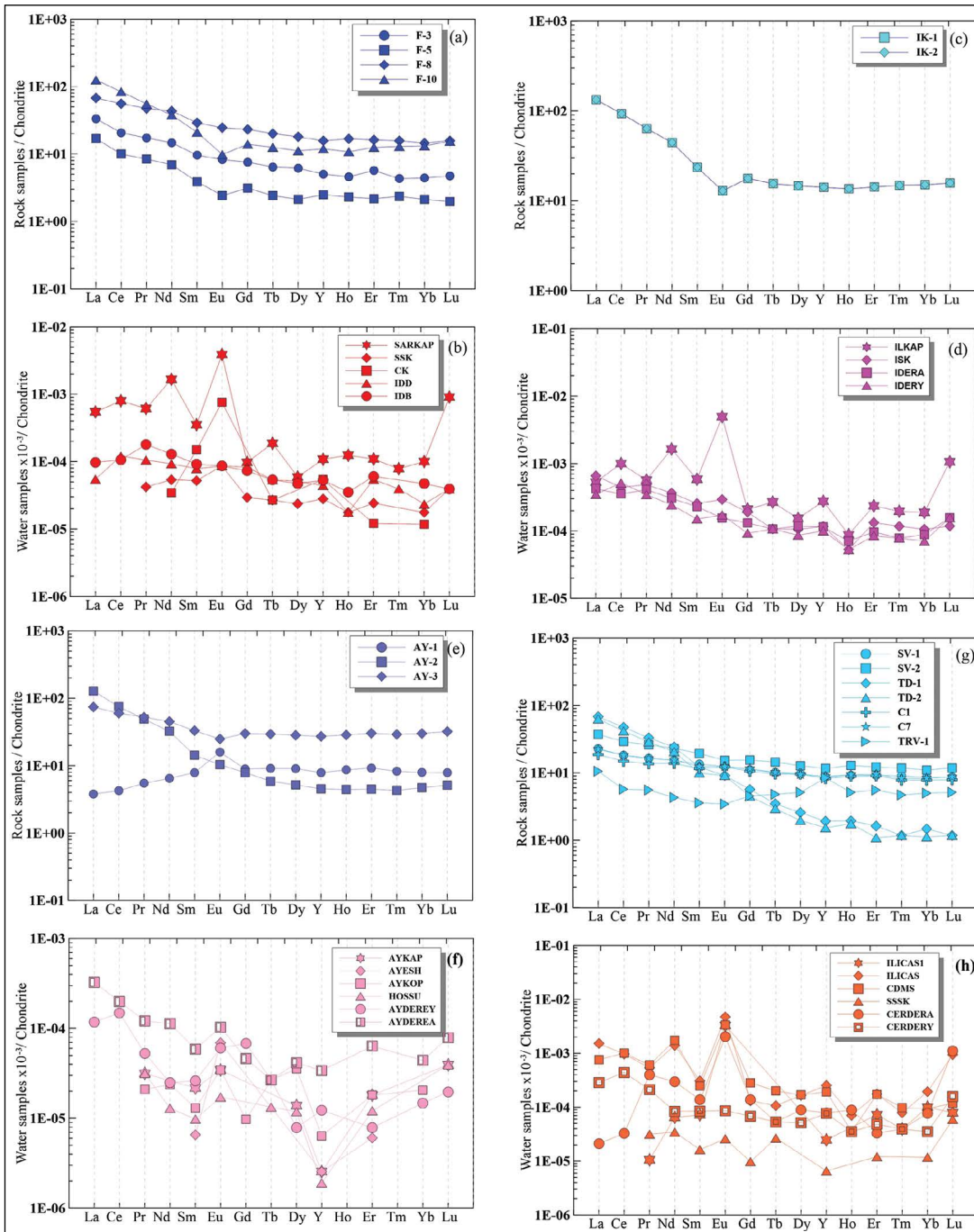
Figure 4- Distribution of Chondrite-normalized REE patterns of rocks (a, c, e and g) and waters (b, d, f and h) (Sun and McDonough, 1989) (a, b:Sarmaşık geothermal fields; c,d: İkizdere geothermal fields; e,f: Ayder geothermal fields; g,h: Şavşat geothermal fields).

waters in the study area (Sun and McDonough, 1989). These ratios show that the majority of the waters are enriched in the Light Rare Earth Elements (La-Eu, LREE) whereas they are poor in terms of the Heavy Rare Earth Elements (Gd-Lu, HREE) (Figures 4b, d, f and h). Similar to many other studies in the literature

in recent years (Gammons et al., 2005; Shakeri et al., 2015; Zhang et al., 2016; Bragin et al., 2018) the TDS amounts and ∑REE values have increased in SGF, IGF and AGF waters with increasing temperature. AGF waters, which are basic in character (pH ~9) compared to other sites, have very low TDS amounts

147

(~97 mg/L) despite the measured high temperature (55°C). The clay minerals, which formed as a result of the argillization of feldspars observed in granitic host rocks within the waters in this field, to absorb elements in the water have caused the decrease of TDS amount of waters and accordingly very low ∑REE concentration.

The most common feature of all the geothermal waters analyzed (except for the Ayder area) is that they have a distinct Eu anomaly. The Eu anomalies calculated in geothermal waters (Eu/Eu*) are 20.84 in SGF, 14.13 in IGF and 23.34 in ŞGF. In the case of AGF, the Eu anomaly was calculated around 3.057 only in the AYKÖPK sample. In addition, the positive Ce anomalies observed in the geothermal waters examined (Sarmaşık: 1.37, İkizdere: 1.81, Şavşat: 1.07, Ayder: not calculated) reflect the reducing conditions in the hydrothermal system. Desorption of Fe oxyhydroxides in hot waters explains high saturation values (Figure 3) and positive Ce anomalies to Fe minerals such as goethite.

The REE+Y contents of the surface water and cold springs in the study areas are changing parallel to the thermal waters in lower concentrations. The fractionation between LREE and HREE concentrations in surface waters is less than that of the geothermal waters.

REE+Y distribution models determined in host rocks in the investigated areas are shown in figures 4a, c, e and g. Tuffite, (F-3), sandy limestone (F-5), basaltic tuff and basalts (F-8, F-10) in SGF, granitic (IK-1, IK-2) and granodioritic (AY-1, AY-2) host rocks, sandstone (SV-1, SV-2), trachyandesite (TD-1, TD-3), volcanogenic sandstone (C1-C7) and travertine (TRV-1) type rocks at İkizdere and Ayder geothermal fields show negative Eu and less distinct Ce anomaly. In addition to these, while the host rocks are enriched in LREE similar to waters they are depleted in HREE.

## 6. Cerium and Europium Anomalies

In the absorption process $Ce^{3+}$ is easily oxidized to $Ce^{4+}$ in iron hydroxides (Bau and Dulski, 1999). Ce anomalies depend on pH and, are observed in alkaline waters (Moller, 2001). Since the $Ce^{4+}$ is preferably adsorbed by Mn oxides (De Carlo et al., 1998), the low temperature surface waters generally show negative Ce anomalies compared to +3 valence REE.

Analyzes of REE+Y behaviors in studies conducted worldwide showed the presence of positive Eu anomaly in high temperature chlorine systems (T>230°C, pH<7). The REE+Y distribution models in these systems are similar, and are not affected by the host rock types. On the other hand, the hydrothermal systems with pH>7 show significant negative Eu anomaly (Klinkhammer et al., 1994). The thermodynamic calculations showed that Eu had a +2 valence in high-temperature fluids (T>300°C) and formed chloride complexes. These complexes are more stable than the complexes formed with +3 valence REE (Haas et al., 1995).

Many studies have shown that REE+Y (especially Eu) fractionation is a complex process, and the behavior of these elements is dependent on the physicochemical environmental parameters (Bragin et al., 2018). REE+Y contents and fractionation of the aquifer composition in high-temperature hydrothermal reservoirs are subject to less impact and consequently the pH and pressure cause the occurrence of complex compound formation (Hass et al., 1995). In low temperature hydrothermal areas close to the surface (T<100°C), the REE+Y contents and distributions are controlled by pH, rock composition and water/rock ratio.

All waters in the study area show a less distinct Ce anomaly (Ce / Ce * = $Ce_{CN}$ / ($La_{CN}$ * $Pr_{CN}$) 0.5) and distinctively positive Eu (Eu / Eu * = $Eu_{CN}$ / ($Sm_{CN}$ * $Gd_{CN}$) 0.5) anomaly except for AGF (Figure 4). It is considered that Eu anomaly originated from the Eu rich minerals (plagioclase ± K-feldspar) present in host rocks of geothermal fields. Ce anomalies in water and host rocks are compatible with each other.

## 7- Transportation Routes of the Rare Earth Elements

REE concentrations in the groundwater are mostly dependent on the solubility of minerals containing REE in the host rock and the degree of decomposition of the host rock. The duration of contact of water with the host rock, the absorption processes and chemical complexation reactions are effective in transporting REE to water. The visual MINTEQ (Gustafsson, 2012) software was used to determine REE transportation processes in the investigated areas. The thermodynamic calculations showed that $Ln^{3+}$, $LnOH^{2+}$, $LnCl^+$, $Ln(SO_4)_2^-$, $LnSO_4^+$, $LnHCO_3^{2+}$,

$Ln(CO_3)_2^-$ and $LnCO_3^+$ complexes were present for each type of REE. The results of the derivation model where the contribution of the major aqueous species of the total dissolved REE to the geothermal and cold springs are shown as the percentage for all studied areas is given in table 5.

Table 5- REE transportation types in hot and cold waters in the study areas (values < 0.05 %).

| | SARKAP | SSK | ILKAP | ISK | AYKAP | AYESH | AYKOPK | HOŞSU | ILICAS | SSSK | CDMS |
|---|---|---|---|---|---|---|---|---|---|---|---|
| $La^{3+}$ | 8.62 | 90.20 | 38.96 | 95.44 | 0.23 | 68.90 | 0.43 | 93.65 | 44.68 | 93.27 | 76.39 |
| $LaOH^{2+}$ | 2.16 | 3.39 | 1.36 | 1.27 | 1.84 | 9.56 | 1.38 | 1.98 | 0.40 | 1.54 | 0.03 |
| $LaCl^{2+}$ | 0.03 | 0.01 | 0.57 | - | - | - | - | - | 1.28 | - | 1.49 |
| $La(SO_4)_2^-$ | 15.94 | - | 3.82 | - | - | 0.09 | 0.05 | - | 0.67 | - | 0.33 |
| $LaSO_4^+$ | 59.83 | 6.39 | 51.31 | 3.28 | 0.37 | 21.44 | 1.02 | 4.37 | 22.49 | 5.19 | 21.76 |
| $LaHCO_3^{2+}$ | 0.16 | - | 0.53 | - | 0.03 | - | 0.02 | - | 5.23 | - | - |
| $La(CO_3)_2^-$ | 0.49 | - | 0.01 | - | 61.63 | - | 54.37 | - | 0.55 | - | - |
| $LaCO_3^+$ | 12.77 | - | 3.43 | - | 35.90 | - | 42.73 | - | 24.70 | - | - |
| $Ce^{3+}$ | 7.31 | 86.17 | 35.33 | 93.97 | 0.09 | 59.44 | 0.17 | 91.49 | 34.36 | 91.74 | 76.52 |
| $CeOH^{2+}$ | 7.92 | 7.79 | 6.54 | 2.85 | 3.41 | 22.13 | 1.81 | 4.32 | 1.15 | 3.27 | 0.07 |
| $CeCl^{2+}$ | 0.03 | 0.01 | 0.46 | - | - | - | - | - | 0.99 | - | 1.79 |
| $Ce(SO_4)_2^-$ | 8.07 | - | 2.01 | - | - | 0.05 | 0.01 | - | 0.32 | - | 0.22 |
| $CeSO_4^+$ | 52.18 | 6.02 | 48.53 | 3.17 | 0.15 | 18.37 | 0.41 | 4.18 | 17.60 | 4.99 | 21.40 |
| $CeHCO_3^{2+}$ | 0.13 | - | 0.45 | - | - | - | - | - | 3.75 | - | - |
| $Ce(CO_3)_2^-$ | 1.21 | - | 0.03 | - | 67.30 | - | 61.67 | - | 1.21 | - | - |
| $CeCO_3^+$ | 23.16 | - | 6.65 | - | 29.06 | - | 35.93 | - | 40.62 | - | - |
| $Pr^{3+}$ | 6.59 | 85.60 | 34.38 | 93.71 | 0.05 | 58.60 | 0.09 | 91.09 | 28.58 | 91.42 | 76.60 |
| $PrOH^{2+}$ | 6.97 | 8.41 | 6.00 | 3.12 | 1.74 | 23.25 | 1.01 | 4.74 | 0.96 | 3.61 | 0.08 |
| $PrCl^{2+}$ | 0.03 | 0.01 | 0.45 | - | - | - | - | - | 0.82 | - | 1.79 |
| $Pr(SO_4)_2^-$ | 6.14 | - | 1.92 | - | 0.08 | 0.03 | - | - | 0.20 | - | 0.11 |
| $PrSO_4^+$ | 47.03 | 5.98 | 47.24 | 3.16 | - | 18.11 | 0.22 | 4.16 | 14.64 | 4.97 | 21.42 |
| $PrHCO_3^{2+}$ | 0.10 | - | 0.38 | - | - | - | - | - | 2.72 | - | - |
| $Pr(CO_3)_2^-$ | 2.27 | - | 0.06 | - | 75.16 | - | 69.86 | - | 2.11 | - | - |
| $PrCO_3^+$ | 30.87 | - | 9.57 | - | 22.97 | - | 28.81 | - | 49.97 | - | - |
| $Nd^{3+}$ | 5.92 | 82.38 | 32.24 | 92.31 | 0.04 | 53.15 | 0.08 | 89.03 | 26.64 | 89.77 | 77.42 |
| $NdOH^{2+}$ | 7.96 | 11.68 | 6.84 | 4.49 | 1.78 | 29.71 | 1.13 | 6.80 | 1.17 | 5.23 | 0.12 |
| $Nd(SO_4)_2^-$ | 6.91 | - | 1.99 | - | - | 0.05 | - | - | 0.25 | - | 0.21 |
| $NdSO_4^+$ | 45.49 | 5.94 | 48.40 | 3.20 | 0.07 | 17.09 | 0.19 | 4.18 | 14.55 | 5.00 | 22.26 |
| $NdHCO_3^{2+}$ | 0.10 | - | 0.38 | - | - | - | - | - | 2.72 | - | - |
| $Nd(CO_3)_2^-$ | 2.51 | - | 0.07 | - | 76.71 | - | 71.62 | - | 2.42 | - | - |
| $NdCO_3^+$ | 31.12 | - | 10.07 | - | 21.39 | - | 26.94 | - | 52.26 | - | - |
| $Sm^{3+}$ | 4.75 | 70.12 | 29.48 | 86.15 | 0.02 | 38.05 | 0.04 | 80.19 | 20.23 | 82.51 | 76.85 |
| $SmOH^{2+}$ | 10.97 | 24.71 | 9.46 | 10.79 | 1.34 | 49.40 | 1.10 | 15.96 | 1.66 | 12.79 | 0.29 |
| $Sm(SO_4)_2^-$ | 4.44 | - | 1.30 | - | - | 0.04 | - | - | 0.17 | 4.70 | 0.25 |
| $SmSO_4^+$ | 37.34 | 5.17 | 45.27 | 3.06 | 0.03 | 12.52 | 0.10 | 3.85 | 11.31 | - | 22.61 |
| $SmHCO_3^{2+}$ | 0.09 | - | 0.40 | - | - | - | - | - | 2.37 | - | - |
| $Sm(CO_3)_2^-$ | 4.62 | - | 0.15 | - | 83.27 | - | 79.10 | - | 4.20 | - | - |
| $SmCO_3^+$ | 37.79 | - | 13.94 | - | 15.34 | - | 19.66 | - | 60.07 | - | - |
| $Eu^{3+}$ | 3.95 | 67.46 | 26.96 | 84.80 | - | 34.90 | 0.03 | 78.40 | 17.78 | 81.08 | 75.30 |
| $EuOH^{2+}$ | 11.77 | 27.55 | 11.56 | 12.19 | 0.74 | 53.55 | 0.96 | 17.84 | 1.83 | 14.29 | 0.33 |
| $EuCl^{2+}$ | 0.02 | 0.01 | 0.35 | - | - | - | - | - | 0.51 | - | 1.76 |
| $Eu(SO_4)_2^-$ | 7.80 | - | 2.58 | - | - | 0.06 | - | - | 0.30 | - | 0.46 |
| $EuSO_4^+$ | 31.09 | 4.98 | 41.41 | 3.01 | 0.01 | 11.48 | 0.07 | 3.76 | 9.94 | 4.62 | 22.15 |
| $EuHCO_3^{2+}$ | 0.15 | - | 0.92 | - | - | - | - | - | 3.63 | - | - |
| $Eu(CO_3)_2^-$ | 8.42 | - | 0.41 | - | 91.46 | - | 83.90 | - | 6.64 | - | - |
| $EuCO_3^+$ | 36.80 | - | 15.82 | - | 7.78 | - | 15.05 | - | 59.37 | - | - |
| $Gd^{3+}$ | 4.82 | 72.28 | 28.62 | 87.64 | 0.02 | 39.02 | 0.04 | 82.41 | 22.18 | 84.58 | 76.51 |
| $GdOH^{2+}$ | 15.04 | 22.50 | 14.36 | 9.32 | 2.22 | 48.40 | 1.39 | 13.72 | 2.23 | 10.71 | 0.25 |

Table 5- (continue)

| | | | | | | | | | | | |
|---|---|---|---|---|---|---|---|---|---|---|---|
| GdCl$^{2+}$ | - | - | 0.20 | - | - | - | - | - | 0.34 | - | 0.96 |
| Gd(SO$_4$)$_2^-$ | 6.17 | - | 1.80 | - | - | 0.04 | - | - | 0.24 | - | 0.29 |
| GdSO$_4^+$ | 37.04 | 5.21 | 42.96 | 3.04 | 0.04 | 12.54 | 0.11 | 3.87 | 12.12 | 4.71 | 22.00 |
| Gd(CO$_3$)$_2^-$ | 4.18 | - | 0.13 | - | 83.10 | - | 79.57 | - | 4.11 | - | - |
| GdCO$_3^+$ | 32.65 | - | 11.52 | - | 14.62 | - | 18.89 | - | 56.06 | - | - |
| GdHCO$_3^{2+}$ | 0.10 | - | 0.41 | - | - | - | - | - | 2.72 | - | - |
| Tb$^{3+}$ | 4.27 | 63.69 | 27.57 | 82.90 | 0.01 | 30.63 | 0.02 | 75.94 | 19.37 | 79.25 | 77.65 |
| TbOH$^{2+}$ | 19.24 | 31.86 | 19.27 | 14.30 | 1.69 | 59.87 | 1.15 | 20.59 | 2.88 | 16.44 | 0.41 |
| Tb(SO$_4$)$_2^-$ | 4.58 | - | 1.50 | - | - | 0.03 | - | - | 0.18 | - | 0.23 |
| TbSO$_4^+$ | 30.46 | 4.45 | 37.88 | 2.80 | 0.02 | 9.47 | 0.05 | 3.47 | 9.92 | 4.31 | 21.72 |
| TbHCO$_3^{2+}$ | 0.11 | - | 0.50 | - | - | - | - | - | 2.99 | - | - |
| Tb(CO$_3$)$_2^-$ | 7.38 | - | 0.25 | - | 89.06 | - | 86.66 | - | 7.16 | - | - |
| TbCO$_3^+$ | 33.96 | - | 13.04 | - | 9.22 | - | 12.11 | - | 57.51 | - | - |
| Dy$^{3+}$ | 3.69 | 63.71 | 24.60 | 83.30 | - | 29.63 | 0.02 | 76.60 | 16.43 | 80.13 | 79.20 |
| DyOH$^{2+}$ | 22.75 | 32.20 | 26.06 | 14.12 | 1.83 | 61.87 | 1.03 | 20.20 | 3.11 | 15.90 | 0.41 |
| Dy(SO$_4$)$_2^-$ | 2.55 | - | 0.98 | - | - | 0.01 | - | - | 0.09 | - | 0.10 |
| DySO$_4^+$ | 25.30 | 4.09 | 32.91 | 2.58 | 0.01 | 8.49 | 0.04 | 3.20 | 8.00 | 3.97 | 20.29 |
| DyHCO$_3^{2+}$ | 0.10 | - | 0.49 | - | - | - | - | - | 2.78 | - | - |
| Dy(CO$_3$)$_2^-$ | 8.61 | - | 0.30 | - | 89.50 | - | 87.50 | - | 8.19 | - | - |
| DyCO$_3^+$ | 37.00 | - | 14.65 | - | 8.65 | - | 11.41 | - | 61.41 | - | - |
| Ho$^{3+}$ | 3.81 | 59.76 | 26.79 | 80.54 | - | 27.45 | 0.01 | 72.78 | 16.49 | 76.71 | 79.82 |
| HoOH$^{2+}$ | 19.98 | 36.57 | 21.39 | 17.09 | 1.20 | 65.03 | 0.85 | 24.31 | 2.88 | 19.66 | 0.52 |
| Ho(SO$_4$)$_2^-$ | 2.97 | - | 1.14 | - | - | 0.02 | - | - | 0.10 | - | 0.13 |
| HoSO$_4^+$ | 24.92 | 3.67 | 34.22 | 2.38 | 0.01 | 7.51 | 0.03 | 2.91 | 7.66 | 3.63 | 19.53 |
| HoHCO$_3^{2+}$ | 0.10 | - | 0.48 | - | - | - | - | - | 2.54 | - | - |
| Ho(CO$_3$)$_2^-$ | 10.93 | - | 0.41 | - | 91.73 | - | 89.80 | - | 10.11 | - | - |
| HoCO$_3^+$ | 37.30 | - | 15.58 | - | 7.04 | - | 9.30 | - | 60.22 | - | - |
| Er$^{3+}$ | 3.45 | 56.73 | 26.23 | 78.40 | - | 25.47 | 0.01 | 69.98 | 14.66 | 74.18 | 79.68 |
| ErOH$^{2+}$ | 18.25 | 39.79 | 20.22 | 19.29 | 0.91 | 67.54 | 0.70 | 27.23 | 2.66 | 22.31 | 0.60 |
| Er(SO$_4$)$_2^-$ | 3.81 | - | 1.49 | - | - | 0.02 | - | - | 0.13 | - | 0.23 |
| ErSO$_4^+$ | 22.57 | 3.48 | 33.51 | 2.31 | - | 6.97 | 0.02 | 2.79 | 6.81 | 3.51 | 19.50 |
| ErHCO$_3^{2+}$ | 0.09 | - | 0.51 | - | - | - | - | - | 2.42 | - | - |
| Er(CO$_3$)$_2^-$ | 13.05 | - | 0.52 | - | 92.87 | - | 91.05 | - | 11.84 | - | - |
| ErCO$_3^+$ | 38.78 | - | 17.52 | - | 6.21 | - | 8.22 | - | 61.47 | - | - |
| Tm$^{+3}$ | 2.87 | 50.84 | 22.98 | 74.44 | - | 20.93 | - | 65.19 | 12.50 | 70.10 | 78.27 |
| TmOH$^{2+}$ | 22.25 | 46.03 | 27.14 | 23.36 | 0.98 | 73.33 | 0.70 | 32.21 | 3.23 | 26.57 | 0.75 |
| TmCl$^{2+}$ | - | - | 0.26 | - | - | - | - | - | 0.31 | - | 1.59 |
| Tm(SO$_4$)$_2^-$ | 2.84 | - | 1.10 | - | - | 0.02 | - | - | 0.11 | - | 0.24 |
| TmSO$_4^+$ | 18.76 | 3.12 | 29.36 | 2.20 | - | 5.73 | 0.02 | 2.60 | 5.81 | 3.32 | 19.15 |
| TmHCO$_3^{2+}$ | 0.08 | - | 0.48 | - | - | - | - | - | 2.21 | - | - |
| Tm(CO$_3$)$_2^-$ | 15.32 | - | 0.65 | - | 93.80 | - | 92.35 | - | 14.26 | - | - |
| TmCO$_3^+$ | 37.88 | - | 18.03 | - | 5.22 | - | 6.93 | - | 61.57 | - | - |
| Yb$^{3+}$ | 2.46 | 40.34 | 22.10 | 65.17 | - | 15.50 | - | 54.23 | 10.18 | 59.73 | 79.19 |
| YbOH$^{2+}$ | 22.11 | 57.36 | 27.17 | 33.04 | 0.98 | 80.59 | 0.85 | 43.76 | 3.27 | 37.62 | 1.22 |
| YbCl$^{2+}$ | - | - | 0.20 | - | - | - | - | - | 0.20 | - | 1.28 |
| Yb(SO$_4$)$_2^-$ | 3.07 | - | 1.33 | - | - | 0.02 | - | - | 0.11 | - | 0.31 |
| YbSO$_4^+$ | 14.30 | 2.29 | 24.68 | 1.79 | - | 3.89 | 0.01 | 2.02 | 4.24 | 2.64 | 18.00 |
| Yb(CO$_3$)$_2^-$ | 14.10 | - | 0.67 | - | 92.54 | - | 90.57 | - | 12.46 | - | - |
| YbCO$_3^+$ | 43.89 | - | 23.39 | - | 6.48 | - | 8.56 | - | 67.69 | - | - |
| YbHCO$_3^{2+}$ | 0.07 | - | 0.47 | - | - | - | - | - | 1.85 | - | - |
| Lu$^{3+}$ | 2.63 | 41.88 | 23.79 | 66.56 | - | 16.39 | - | 55.75 | 10.99 | 61.18 | 80.58 |
| LuOH$^{2+}$ | 21.75 | 55.90 | 26.84 | 31.73 | 0.78 | 79.75 | 0.69 | 42.32 | 3.27 | 36.29 | 1.17 |
| LuCl$^{2+}$ | - | - | 0.14 | - | - | - | - | - | 0.14 | - | 0.82 |
| Lu(SO$_4$)$_2^-$ | 2.93 | - | 1.21 | - | - | 0.02 | - | - | 0.11 | - | 0.34 |
| LuSO$_4^+$ | 14.22 | 2.22 | 24.79 | 1.70 | - | 3.84 | 0.01 | 1.93 | 4.27 | 2.52 | 17.10 |
| LuHCO$_3^{2+}$ | 0.07 | - | 0.46 | - | - | - | - | - | 1.82 | - | - |
| Lu(CO$_3$)$_2^-$ | 17.66 | - | 0.84 | - | 94.32 | - | 92.80 | - | 15.79 | - | - |
| LuCO$_3^+$ | 40.75 | - | 21.93 | - | 4.90 | - | 6.50 | - | 63.62 | - | - |

In SGF with a pH value of ~8 and a temperature of 47°C, the total dissolved REE in hot waters dominantly formed the sulfate complexes ($LnSO_4^+$). In general, the REE have been transported to the geothermal water with the main anion sulfate. These complexes gradually decreased from LREE (~59-31%; La-Eu) to HREE (~37-14%; Gd-Lu). In this area, it is seen that the free metal ions ($Ln^{3+}$) are dominant in the cold spring in this field (~90-67%; La-Eu, ~72-41%; Gd-Lu).

Similar to the SGF, the total dissolved REE dominantly formed sulfate complexes ($LnSO_4^+$) in the geothermal well water (ILKAP) which has a pH of ~7 and a temperature of 60°C. These complexes gradually decreased from LREE (~51-41%; La-Eu) to HREE (~42-24%; Gd-Lu). In this area, it is seen that free metal ions ($Ln^{3+}$) are dominant in cold spring (~95-84%; La-Eu, ~87-66%; Gd-Lu).

In AGF, the bicarbonate ($LnHCO_3^{2-}$) complexes formed dominant species by increasing with the increased atomic numbers of the REE in the AYKAP geothermal well water with a pH value of ~9 and temperature of 55°C (~61-91%; La-Eu, ~83-94; Gd-Lu). The free metal ions ($Ln^{3+}$) gradually decreased from La to Nd, and formed dominant species in AYESH geothermal spring water with a pH of ~8 and the temperature of 20°C. $LnOH^{2+}$ complexes from Sm to Lu have become dominant by increasing with the increasing atomic number. In the hot spring of AYKOPK (pH: 9.3, temperature: 31.7°C), the carbonate ($LnCO_3^+$) complexes have formed dominant species by increasing with the increasing atomic numbers of REE (~54-83%; La-Eu, ~79-92%; Gd-Lu). The concentrations of carbonate complexes of REE have also increased with high pH values in AGF. The cold spring (HOŞSU) in the field gradually decreases with increasing atom numbers (~93-78%; La-Eu, ~82-55%; Gd-Lu) and form dominant species of free metal ions ($Ln^{3+}$).

In the ILICAS well (pH: 6.9, temperature: 38.8°C) in ŞGF, the carbonate ($LnCO^{3+}$) complexes increased with increasing atom numbers of REE (~44-59%; La-Eu, ~56-63%; Gd-Lu) and formed dominant species. Free metal ions ($Ln^{3+}$) in cold springs in the field decreased with the increasing atomic numbers of the REE in the SSSK spring (pH: 7.5, temperature: 9.2°C) (~93-81%; La-Eu, ~84-61%; Gd-Lu) formed dominant complexes without changing too much

(~76%; La-Eu,: ~79%; Gd-Lu) in the CDMS spring (pH: 6.2, temperature: 12°C).

## 8. Results

The thermal waters located in the Eastern Black Sea Region, which are controlled by tectonic lines in magmatic (plutonic and volcanic) rocks are as follows; SGF thermal waters in Na-Ca-SO$_4$ type with a temperature of 47°C; İGF thermal waters in Na-Ca-HCO$_3$ type with a temperature of 60°C; AGF thermal waters in Na-Ca-CO$_3$-SO$_4$ type with a temperature of 55°C and ŞGF thermal waters in Na-HCO$_3$-Cl type with a temperature of 39°C. The ∑REE contents in these geothermal waters with pH values varying in between 7-9 are at very low (0.02-2.13 ppb) concentrations. The highest ∑REE concentration was determined in the ILKAP (İkizdere) and ILICAS (Şavşat) geothermal waters where the TDS values were also high. Low REE concentrations, typically detected in alkaline thermal waters, were observed in AGF geothermal water with a high pH (8.60-9.86). The REE contents of the cold springs are lower than the geothermal waters and vary between 0.02-0.82 ppb. In the cold water with a high ion content (TDS: 2369 mg/L) in ŞGF, the ∑REE is 2.05 ppb. The ∑REE values in surface waters vary between 0.1-0.64. This situation indicates that the total ion concentration is more effective than the temperature on ∑REE values.

The majority of waters in the studied areas showed LREE/HREE fractionation towards the LREE enrichment. Except for the Ayder area, all geothermal waters have a distinct positive Eu, less significant Ce anomaly. It is considered that the source of Eu anomaly in waters is Eu rich minerals in host rocks of the geothermal areas. The less distinct Ce anomaly in geothermal systems indicates the reducing conditions. According to the calculations of the transport modes, the REEs are transported in the form of $LnSO_4^+$, $LnHCO_3^{2-}$, $LnCO_3^+$ and $Ln^{3+}$ in the AGF and $LnCO_3^+$ and $Ln^{3+}$ complexes in the SGF and IGF. On the other hand, the contents of REE in waters depend on their individual properties, such as the atomic numbers, the temperature and pH of the fluid.

## Acknowledgements

## References

Akkuş, İ., Akıllı, H., Ceyhan, S., Dilemre, A., Tekin, Z. 2005. Türkiye Jeotermal Kaynakları Envanteri, Maden Teknik Arama Genel Müdürlüğü Envanter Serisi-201, Ankara.

Arslan, M., Aslan, Z. 2006. Mineralogy, Petrography and Whole-Rock Geochemistry of the Tertiary Granitic Intrusions in the Eastern Pontides, Turkey, Journal of Asian Earth Sciences, 27, pp.177-193.

Arslan, M., Temizel, İ., Abdioğlu, E., Kolaylı, H., Yücel, C., Boztuğ, D., Şen, C. 2013. "40Ar-39Ar dating, whole-rock and Sr-Nd-Pb isotope geochemistry of post-collisional Eocene volcanic rocks in the southern part of the Eastern Pontides (NE Turkey): Implications for magma evolution in extension-induced origin", Contribution to Mineralogy and Petrology, 166, pp.113-142.

Bau, M., Dulski, P. 1999. Comparing yttrium and rare earths in hydrothermal fluids from the Mid-Atlantic Ridge: implications for Y and REE behaviour during near-vent mixing and for the Y/Ho ratio of proterozoic seawater. Chem Geol 155(1-2): pp.77-90.

Bragin I.V., Kharitonova N.A., Chelnokov, G.A., Aseeva, A.V., Chudaev, O.V. 2018. REY geochemistry in groundwater from Paratunka geothermal area (Kamchatka peninsula, Far East of Russia), Environmental Earth Sciences, 77, 376p.

Büyük, M. 1978. Fatsa (Sarmaşık) Kaplıcası Hidrojeoloji Etüdü, Maden Tetkikve Arama Genel Müdürlüğü Rapor No: 6082, Ankara (unpublished).

Craddock, P.R, Bach, W. 2010. Insights to magmatic-hydrothermal processes in the Manus back-arc basin as recorded by anhydrite. Geochim Cosmochim Acta 74(19): pp.5514–5536.

De Carlo, E.H., Wen, X.Y., Irving, M.1998. The influence of redox reactions on the uptake of dissolved Ce by suspended Fe and Mn oxide particles. Aquat. Geochem. 3, pp.357–389.

Embley, R.W., Baker, E.T., Butterfield, D.A., Chadwick, W.W., Lupton, J,E., Resing, J.A., de Ronde, C.E.J., Nakamura, K.I., Tunnicliffe, V., Dower, J.F., Merle, S.G. 2007. Exploring the submarine ring of fire: Mariana Arc—Western Pacific. Oceanography 20(4): pp.68–79

Erzenoğlu, Z., Tangaç, Ö.F. 1986. Ordu- Fatsa (Sarmaşık) Kaplıcası Ilıca-1 Sıcak Su Sondajı Kuyu Bitirme Raporu: Maden Tetkik ve Arama Genel Müdürlüğü Rapor No: 7890, 11p. Ankara (unpublished).

Evcimen, Ö., Karslı, O. 2012. İkizdere Plütonu'nun (KD Türkiye) U-Pb Jeokronolojisi, Petrolojisi ve Jeodinamik Önemi, 65.Türkiye Jeoloji Kurultayı 2-6 Nisan/April, 366p.

Fırat Ersoy, A. 2001. Ilıcaköy (İkizdere-Rize) Sıcak Su Kaynaklarının Hidrojeolojisi, (MSc Thesis), Karadeniz Teknik Üniversitesi Fen Bilimleri Enstitüsü.

Gammons C.H., Wood, S.A., Pedrozo, F., Varekamp, J.C., Nelson, B.J., Shope, C.L., Baffico, G. 2005. Hydrochemistry and rare earth element behavior in a volcanically acidified watershed in Patagonia, Argentina. Chem Geol 222: pp.249-267

Gedik, A., Ercan, T., Korkmaz, S., Karataş, S. 1992. Rize- Fındıklı- Çamlıhemşin Arasında (Doğu Karadeniz) Yer Alan Magmatik Kayaçların Petrolojisi ve Doğu Pontidlerdeki Bölgesel Yayılımları, Türkiye Jeoloji Bülteni, C. 35, pp.15-38, Ankara.

Göb, S., Loges, A., Nolde, N., Bau, M., Jacob, D.E., Markl, G. 2013. Major and trace element compositions (including REE) of mineral, thermal, mine and surface waters in SW Germany and implications for water– rock interaction. Appl Geochem 33: pp.127-152.

Göksu, E. 1996. 1/500.000 ölçekli Türkiye Jeoloji Haritası Samsun Paftası açıklaması, Maden Tetkik ve Arama Genel Müdürlüğü yayını, Ankara.

Gustafsson, J.P. 2012. Visual MINTEQ ver. 3.0. Dept of Land and Water Resources Engineering, Stochholm, Sweden (E-mail: gustafjp@kth.se).

Güven, İ. H. 1993. "Doğu Pontidler'in 1/250.000 Ölçekli Kompilasyonu", Maden Tetkik ve Arama Genel Müdürlüğü, Ankara.

Gürsel, F. 1991. Ayder (Çamlıhemşin-Rize) ve Çevresinin Jeotermal Enerji Yönünden İncelemesi, (MSc Thesis), Karadeniz Teknik Üniversitesi Fen Bilimleri Enstitüsü.

Gündüz, M. 1999. Rize-İkizdere-Ilıcaköy Sıcaksu Sahası Hidrojeoloji İncelemesi, (MSc Thesis) Hacettepe Üniversitesi, Fen Bilimleri Enstitüsü.

Haas, J.R., Shock, E.L., Sassani, D.S.1995. Rare earth elements in hydrothermal systems: estimates of standard partial molar thermodynamic properties of aqueous complexes of the rare earth elements at high pressures and temperatures. Geochim Cosmochim Acta 59: pp.4329–4350.

Kara, İ. 1997. Türkiye Termal Ve Mineralli Sular Envanteri (Artvin) Maden Tetkik ve Arama Genel Müdürlüğü Rapor No: 10261, 19p. Ankara (unpublished).

Kartal, T. 1972. Rize-Ayder Kaplıcası Hidrojeoloji Raporu: Maden Tetkik ve Arama Genel Müdürlüğü Rapor No: 5689, 20p. Ankara (unpublished).

Karslı, O., Aydın, F., Sadıklar, M.B. 2004. The Morphology and Chemistry of K-Feldspar Megacrysts from Ikizdere Pluton: Evidence for Acid and Basic Magma Interactions in Granitoid Rocks, NE-Turkey: Chemie der Erde-Geochemistry 64, pp.155-170.

Ketin, İ. 1966. Anadolu'nun tektonik birlikleri. Maden Tetkik ve Arama Dergisi no. 66, pp.20-34, Ankara.

Klinkhammer, G., German, C.R., Elderfield, H., Greaves, M.J., Mitra, A. 1994. Rare earth elements in hydrothermal fluids and plume particulates by inductively coupled plasma mass spectrometry. Mar Chem 45 (3): pp.179–186

Moller, P. 2001. The behavior of REE and Y in water-rock interactions. Water-Rock Interaction. In: Proceedings of the 10th International Symposium. Rotterdam: Balkema, Netherlands, vol 2, pp.989-992.

Okay, A. İ., Tüysüz, O. 1999. "Tethyan sutures of northern Turkey", In: Durand, B., Jolivet, L., Hovarth, F., Séranne, M. (eds), The Mediterranean Basins: Tertiary Extension within the Alpine Orogen Tethyan Sutures of Northern Turkey. Geological Society, London, Special Publications, 156, pp.475-515.

Özbeşikçi, A., Kırcı, M., Uysal, M. 1981. Ordu–Giresun–Gümüşhane-Samsun Yörelerindeki Manganez Zuhurlarına Ait Prospeksiyon Rapor no: 7162, Maden Tetkik ve Arama Genel Müdürlüğü. Ankara (unpublished).

Özsayar, T., Pelin, S., Gedikoğlu, A. 1981. Doğu Pontidlerde Kretase, KTÜ., Yerbilimleri Dergisi, 2, pp.65-114.

Shakeri, A., Ghoreyshinia, S., Mehrabi, B., Delavari, M. 2015. Rare earth elements geochemistry in springs from Taftan geothermal area SE Iran. J Volcanol Geotherm Res 304: pp.49-61.

Sun, S.S., McDonough, W.F. 1989. Chemical and isotopic systematics of oceanic basalts; implications for mantle composition and processes. In: Magmatism in the ocean basins. Saunders, A.D. and Norry, M.J. (Editors), Geological Society of London, London. 42: pp.313-345.

Terlemez, İ., Yılmaz, A. 1980. Ünye-Ordu-Koyulhisar-Reşadiye Arasında Kalan Yörenin Stratigrafisi, TJK Bülteni, 23/2, pp.179-192, Ankara.

Temizel, İ., 2002. İkizce (Ünye-Ordu) Yöresi Volkanik Kayaçlarının Petrografik, Jeokimyasal ve Petrolojik İncelenmesi, (MSc Thesis), Karadeniz Teknik Üniversitesi Fen Bilimleri Enstitüsü, Trabzon.

Temizel, İ., Arslan, M., Ruffet, G. Peucat, J.J. 2012. Petrochemistry, Geochronology and Sr–Nd İsotopic Systematics Of The Tertiary Collisional And Post-Collisional Volcanic Rocks From The Ulubey (Ordu) Area, Eastern Pontide, Ne Turkey: Implications For Extension-Related Origin And Mantle Source Characteristics, Lithos, 128, pp.126-147.

Temizel, İ., Arslan, M., Yücel, C., Abdioğlu, E., Ruffet, G. 2016. "Geochronology and geochemistry of Eocene-aged volcanic rocks around the Bafra (Samsun, N Turkey) area: Constraints for the interaction of lithospheric mantle and crustal melts", Lithos, 258-259, pp.92-114.

Uzel, Ö. F., Gündüz, M. 1998. Yıldız, S., Rize- İkizdere Kaplıcası sıcak su sondajı Ilıcaköy-1 ve Ilıcaköy-2 kuyu bitirme raporu: Maden Tetkik ve Arama Genel Müdürlüğü Rapor No: 10213, 11p. Ankara (unpublished).

Wood, S, A. 1990. The aqueous geochemistry of the rare-earth elements and yttrium. 1. Review of available low-temperature data for inorganic complexes and the inorganic REE speciation of natural waters. Chem Geol 82(C): pp.159-186.

Yücel, C. 2013. "Trabzon-Giresun arasındaki Tersiyer volkanitlerinin petrografisi, 40Ar-39Ar jeokronolojisi, petrokimyası, Sr-Nd-Pb izotop jeokimyası ve petrolojisi", Karadeniz Teknik Üniversitesi, Fen Bilimleri Enstitüsü, PhD Thesis, 406p.

Zhang, Y., Tan, H., Zhang, W., Wei, H., Dong, T. 2016 Geochemical constraint on origin and evolution of solutes in geothermal springs in western Yunnan, China. Chemie der Erde, 76, pp.63-75.